Journal of
Materials Chemistry A

Accepted Manuscript

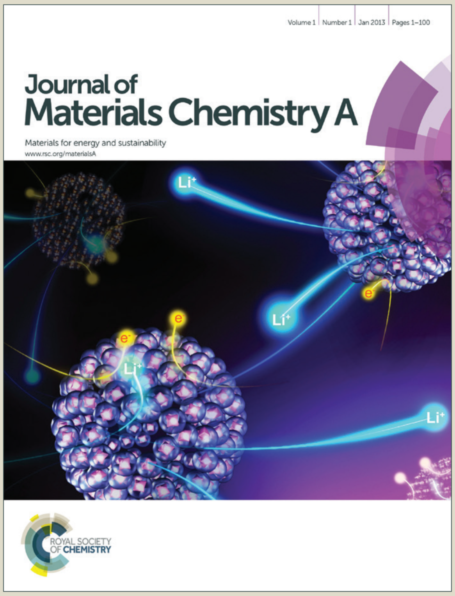

ROYAL SOCIETY
OF CHEMISTRY

www.rsc.org/materialsA

Cite this: DOI: 10.1039/c0xx00000x

www.rsc.org/xxxxxx

ARTICLE TYPE

Direct Growth of Mesoporous Carbon-coated Ni Nanoparticles on Carbon Fibers for Flexible Supercapacitors

Jun Li,[a,b] Yuhang Wang,[a] Jing Tang,[a] Yang Wang,[a] Tianyu Wang,[a] Lijuan Zhang,[a] and Gengfeng Zheng*[a]

Received (in XXX, XXX) Xth XXXXXXXXX 20XX, Accepted Xth XXXXXXXXX 20XX
DOI: 10.1039/b000000x

We demonstrated a facile solution method for direct growth of mesoporous carbon-coated nickel nanoparticles on conductive carbon blacks (CCBs) treated carbon fibers (CFs), using an oleate-assisted deposition/calcinations process. The obtained composite has a uniform Ni core of ~ 5−10 nm, and a carbon surface layer of ~2 nm, which avoids aggregation and pulverization of inner nanoparticles and serves as a protective layer of Ni cores from dissolution during electrochemical reactions. In addition, the oleate decomposition during calcination leads to the formation of mesopores, which enable sufficient interaction between electrolyte and inner active materials and provide a high surface area of 71 m^2/g for electrochemical reaction and efficient pathways for electrolyte diffusion. Moreover, the introduction of conductive carbon blacks to carbon fibers substrate significantly reduces the internal resistance and leads to enhanced electrochemical properties. These mesoporous carbon-coated nickel nanoparticles show a high capacitance of ~ 700 F/g at 1 A/g current density. The excellent cycling stability over repeated folding cycles for single electrodes and the mechanical stability of different twisted and bent state for solid-state active carbon (AC)//Ni@C asymmetric supercapacitors (ASCs) suggest a potential candidate for flexible energy storage.

Introduction

The rapidly increasing demand for high-power energy utilization has driven substantial research progresses in developing efficient energy storage materials and devices, such as batteries[1-4] and supercapacitors,[5-7] with the capabilities of applying for thin-film, flexible devices.[8-13] The transition metal-based supercapacitors represent a large category of electrochemical energy storage materials, in which the oxides and hydroxides of nickel are among the research foci, due to their high theoretical storage capacity, environmental benignity and low cost.[14] Nonetheless, due to their poor electrical conductivity and structural stability, the device performances, including the rate capability and cycling stability, are still largely limited. Fabrication of hybrid materials is of particular interest for improving the conductivity and stability of Ni-based materials, such as formation of NiO/carbon microsphere assemblies,[15] coating of carbon or polymeric shell layers,[16-18] incorporation of conducting components like graphene,[19,20] and constructing NiO/Co_3O_4 hybrid materials for improved conductivity and capacity.[21-22] In addition to Ni oxide and hydroxide, the use of mesoporous Ni/carbon hybrid structures for electrochemical energy storage has also been reported recently, in which the existence of mesopores allows for high surface area for electrochemical reaction, fast electrolyte transport kinetics, and structural flexibility.[23] For instance, mesoporous Ni/carbon nanotubes were synthesized by an electroless deposition method with a non-ionic surfactant Brij56, where mesoporous Ni nanoparticles were heterogeneously nucleated and grown on the outer surface of carbon nanotubes.[24] By co-assembly of dopamine and block copolymer on the surface of pre-formed $Ni(OH)_2$ nanowires followed by high temperature annealing, peapod-like Ni@mesoporous carbon core-shell nanowires were fabricated, with a high capacitance of 912 F/g at 0.5 A/g current density.[25] However, these approaches involve separate synthetic steps for Ni and carbon materials, as well as the use of surfactant for mesopore formation. Very recently, the synthesis of mesoporous carbon-coated MnO nanoparticles was reported by a facile synthetic strategy, in which the Mn^{2+} salt and oleic acid are reacted through a two-phase solution reaction at room temperature and deposited onto Ni or Ti substrates, followed by annealing to produce mesopores.[26] Nonetheless, the direct growth of metal/carbon hybrid structures, with the capability of utilization in flexible energy storage, has yet to be demonstrated.

In this paper, we demonstrate a one-pot synthesis of Ni nanoparticles@mesoporous carbon hybrid structures on flexible carbon fibers, using the oleate-assisted deposition/calcination process. This approach allows for the direct growth of electrochemically active materials on conducting substrates, enabling fast transfer of both charges and ions towards the electrode surface. The fabrication steps are schematically displayed in **Figure 1**. Ni(II) salt and sodium oleate are initially dissolved in aqueous and hexane solutions, respectively, and mixed to form a heterogeneous interface. The self-assembly of oleate reverse micelle leads to the transfer of Ni(II) ions towards the hexane phase and forms Ni(II) oleate. The hexane solution containing Ni(II) oleate can be uniformly coated onto a flexible and conducting substrate, such as CCBs treated CFs. Subsequent thermal treatment in an inert atmosphere degrades Ni(II) oleate into a Ni@C composite, in which Ni nanoparticles are uniformly coated by mesoporous carbon. The Ni nanoparticles provide high surface area for electrolyte contact and electrochemically reactive surface. The mesoporous carbon coating provides entries for electrolyte ions, as well as conduction frameworks for efficient charge transfer. Furthermore, the carbon layer also prevents the aggregation and dissolution of Ni particles during charge/discharge cycles, thus leading to enhanced capacitance and cycling performance. As a proof-of-concept, the Ni nanoparticle@mesoporous carbon (mesoporous Ni@C) composite grown on flexible carbon fiber shows a capacitance of ~ 700 F/g at 1 A/g, with excellent cycling stability over 4500 cycles. Moreover, the whole device can be repeatedly folded and bent with negligible capacitance decrease, indicating the possibility of exploring this fabrication strategy for flexible electrochemical energy storage.

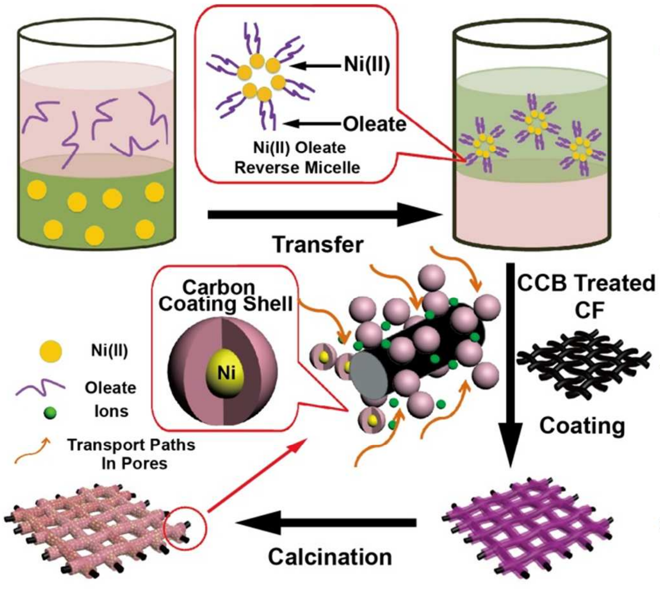

Figure 1. Schematic illustration of the direct growth of mesoporous carbon coated Ni nanoparticles on CCB treated CF.

Experimental

Material synthesis and electrode preparation

For synthesizing the Ni-oleate precursor, a simple chemical reaction of $NiCl_2$ and sodium oleate was performed. 0.95 g of $NiCl_2 \cdot 6H_2O$ (4 mmol), 3.65 g of sodium oleate (12 mmol), 6 mL of de-ionized (DI) water, 8 mL of ethanol and 14 mL of hexane were mixed and magnetically stirred at room temperature for 30 min to obtain two immiscible liquid phases with light green transparent upper solution. The resultant mixture was transferred to an oven and kept still and aged at 70 ^{o}C for 4 h. Afterwards, the upper solution (organic phase) was washed with DI water for three times to evaporate off hexane and obtain the Ni-oleate complex in a waxy solid form. To prepare for the flexible mesoporous Ni@C composite electrode, carbon fibers were employed as substrates and first dipped into a mixture of 0.4 g of conductive carbon blacks and 20 mL of ethanol to decrease the internal resistance and improve the conductivity of substrate. Afterwards, the conductive carbon black treated carbon fibers were dried at room temperature and then dipped into the Ni-oleate precursor solution for several seconds. After evaporating at room temperature, the substrate was coated with a light-green waxy solid. Repeatedly coating for several times could enhance the loading amount of the Ni-oleate precursor. Finally, the resulting products were carbonized and heated to 350 ^{o}C at 10 ^{o}C min^{-1} under N_2 atmosphere, and then kept for 2 h before cooling to room temperature. The mechanism of monodispersed nanoparticle formation was proposed as follows. In brief, the metal oleate, such as Ni(oleate)$_2$, is formed first in the solution reaction. One oleate ligand dissociates from the precursor at 200-240 °C and the remaining two oleate ligands dissociate at ~300 °C by a CO_2 elimination pathway. The oleate ligands thermally reduce Ni^{2+} to Ni^0. In addition, the mesopores were formed during the formation/elimination of CO_2 from the reactants.

Solid-state AC//Ni@C ASCs fabrication

First, the poly(vinyl alcohol) (PVA)/KOH gel electrolyte was prepared as follows: 3 g PVA power were added to 30 mL of DI water, and the mixture was heated up to 85 ^{o}C under vigorous stirring until the solution became clear. Then 20 mL of 6 M KOH was added to form a homogeneous solution. Second, to prepare AC based anode, a mixture containing 80 wt % AC, 10 wt % acetylene black and 10 wt % polytetrafluoroethylene (PTFE) was well mixed and then pressed onto a nickel foam (NF) (1.0×10^7 Pa) that was served as a current collector. The Ni@C on CCB treated CF-based cathode was connected to a Ti foil by Ag colloid. Third, the anode and cathode materials were soaked in PVA/KOH gel electrolyte while care was taken to ensure that one end of each electrode was not contacted with PVA/KOH gel. Finally, the materials were sandwiched in parallel format without the use of a separator and kept still at room temperature for several hours to vaporize the excess water, which formed the solid-state integrated ASCs.

Characterization and electrochemical measurement

The sample morphologies were examined by scanning electron microscopy (SEM) and transmission electron microscopy (TEM). The X-ray diffraction (XRD) patterns of the samples were observed by XRD (Max 18 XCE, Japan) using a Cu Kα (l ¼ 0.1542 nm) at over a 2-theta range of 30–80^{o}. Using energy dispersive analysis by X-ray (EDAX, Link-200, United Kingdom). N2 sorption isotherms were determined by Brunauer-Emmett-Teller (BET) measurements using an ASAP-2010 surface area analyzer. The content of Ni in the nanocomposite was tested by ion-conductive plasma (ICP) following the methods below: an as-prepared mesoporous Ni@C composite sample was dissolved for the Ni content by mixing in HCl (2 M). Then ICP was utilized to measure the supernatant, which showed the concentration of Ni^{2+} and excluded the presence of any other metal ions, thus indicating the purity of our samples. The mass percentage of Ni was then calculated according to the measured Ni^{2+} concentration and the original sample mass.

The electrochemical measurements were carried out by means of an electrochemical analyzer system, CHI660B (CH Instruments Inc., USA) in an electrochemical cell with a working electrode, a platinum plate counter electrode and an Ag/AgCl reference electrode. The electrolyte was a 6 M KOH aqueous solution.

Results and discussion

Physicochemical characterization

After coating of the Ni-oleate solution onto the CCBs treated CFs substrate, it forms a waxy coating on the surface. The coated layer is converted into black color after thermal treatment in N_2, suggesting the formation of carbon during calcinations. Scanning electron microscopy (SEM) images show the nanoparticles spread out evenly on the carbon fiber substrate and closely packed with their neighbors to form a continuous film (**Fig. 2a, b**). The net mass per area coated over the CCBs treated CFs is about 4.5 mg/cm^2. The loading density can be tuned conveniently by the coating times. An almost linear increase of the film mass loading is observed with the coating times, while the loading density is close to saturation after 5 times of repeated coating (**Fig.S1**). Most of the nanoparticles are individually separated by the carbon layer, without being merged into large aggregations (**Fig. 2c, d**). High-resolution TEM (HRTEM) images exhibit that well-resolved lattice fringes (**Fig. 2d** inset). The *d*-spacing values are measured to be 0.203 and 0.174 nm, which are corresponding to the (111) and (200) planes of Ni crystals, indicating the single-crystalline nature of these nearly spherical nanoparticles. The amorphous carbon layer between adjacent nanoparticles is also clearly observed, with an average thickness of 2−3 nm. As many single-crystalline Ni nanoparticles are packed together, the selected area electron diffraction (SAED) pattern displays multiple dot features forming several ring structures, revealing a poly-crystalline diffraction pattern (**Fig. 2e**). The first three diffraction rings of the SAED pattern are in good accord with the (111), (200) and (220) lattice planes. X-ray diffraction (XRD) measured is further carried out to characterize the structure and phase purity of this mesoporous Ni@C composite grown on carbon fibers. Three distinct diffraction peaks at 44.5^o, 51.8 ^{o}, 76.4 ^{o} are observed (**Fig. 2f**), well indexed as the 111, 200 and 220 reflection of Ni crystals (JCPDS No. 65-0380), which are consistent with the HRTEM and SAED results. No other peaks are observed, suggesting the high purity of the obtained Ni nanoparticles.

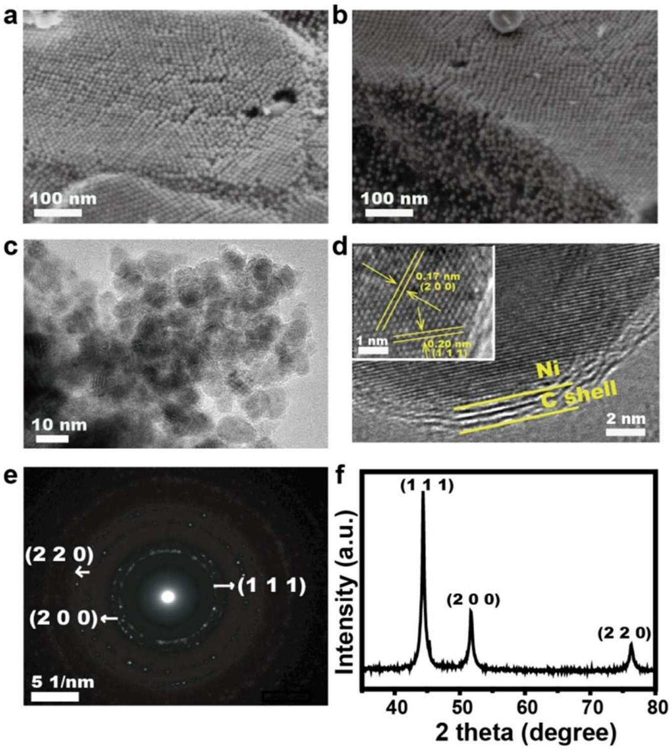

Figure 2. Structure characterization of the mesoporous Ni@C composites directly grown on carbon fibers. (a) Top-view and (b) side-view SEM images; (c) TEM and (d) HRTEM images; (e) SAED pattern; (f) XRD pattern.

X-ray photoelectron (XPS) spectrum of the obtained mesoporous Ni@C composite is performed to study the electronic states of the sample (**Fig. 3a**). A large peak at 853.6 eV and a satellite peak at 859.5 eV are ascribed to the Ni 2p 3/2 levels. Another peak centered at 870.7 eV corresponds to the Ni 2p 1/2 level. All these three peaks fit well with previous literature of Ni XPS peaks,[27] confirming the existence of Ni(0). The porosity of the mesoporous Ni@C composite is investigated by the N_2 sorption isotherm, which shows a typical type-IV curve with a distinct hysteresis loop (**Fig. 3b**). This feature of N_2 sorption isotherm indicates the existence of mesoporous structures in the composite, with a calculated surface area (S_{BET}) as 71 m^2/g. The pore size derived from the adsorption branch shows a wide distribution of large mesopore size between 5−30 nm (**Fig. 3b** inset), corresponding to the stacking pores by the nanoparticles. This high surface area and large mesopore size are beneficial for providing sufficient interface between the electroactive materials and the electrolyte.

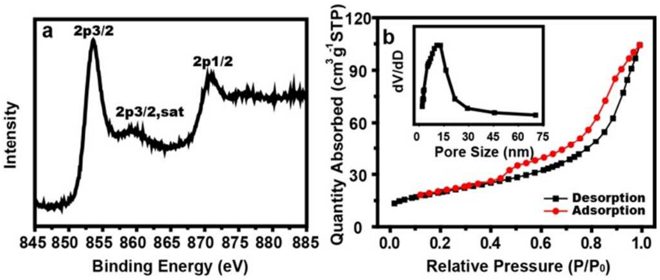

Figure 3. (a) XPS spectra of the mesoporous Ni@C composite. (b) Nitrogen sorption isotherm of the mesoporous Ni@C composite. Inset: pore distribution.

Electrochemical properties

The electrochemical performance of the obtained Ni nanoparticle/mesoporous carbon composite is first studied by the cycle voltammetry (CV) measurement. The conversion from Ni to its corresponding NiO through electrochemical oxidation has been carried out by potential scanning at the nickel oxide region, which includes multiple oxidation states and contributes to the electrochemical performance of Ni nanoparticles.[28,29] Under different scanning rates of 5, 10, 25, 50 and 100 mV s^{-1}, the CV curves of the mesoporous Ni@C composite consist of a pair of strong redox peaks (**Fig. 4a**), indicating that the capacitance characteristics are mainly attributed to Faradic reactions based on the surface redox mechanism.[25] In the oxidation half cycle, the main peak is located at 0.18 V, in good accord with the oxidation of Ni(II) to Ni(III) in previous reports.[30] In the reduction half cycle, a main cathodic peak close to −0.11 V is observed, corresponding to the reduction of Ni(III) to Ni(II).[24] The capacitance contribution from substrate is negligible, as the measured CV curve of the substrate exhibits an extreme small area (**Fig. S2**), compared with that of the mesoporous Ni@C composite. In addition, the shapes of the cyclic voltammograms are retained even at a high potential scan rate of 100 mV s^{-1}, revealing high electrochemical kinetic reversibility of the mesoporous Ni@C composite.

The capacitance of the mesoporous Ni@C composite directly grown on CCB treated CFs is first evaluated by the galvanostatic measurement, which is useful for calculating the supercapacitive performance. The charge and discharge curves of the samples are measured in a potential range of −0.2 to 0.3 V. The potential window is chosen to include the redox peaks, which indicate that the capacitance characteristics are governed by Faradaic reactions based on the surface redox mechanism of Ni(II) to Ni(III). At various current densities, the mesoporous Ni@C composite displays discharge and charge curves with a symmetrical, triangular shape (**Fig. 4b**), suggesting the excellent capacitor behaviors of the electrode. No obvious plateaus correspond to the redox peaks in CV curve are observed, mainly because the substrate is firstly treated by conductive carbon black to reduce the internal resistance. The conductive carbon black and the carbon coating in the Ni@C composites lead to double layer capacitance, and thus a linear variation from -0.2 to 0.2 V is observed.[31] For comparison, the galvanostatic measurement of mesoporous Ni@C composite grown on CFs without CCB treated is performed (**Fig. S3**). Evidently, great voltage (IR) drop and shorter discharge time are observed, confirming the inferior electrical conductivity and electrochemeical performance without extra conductive carbon black. The mesoporous Ni@C composite directly grown on CCB treated CFs electrode demonstrates capacitance values of 702, 673, 637, and 593 F/g, at current densities of 1, 2, 4 and 8 A/g, respectively (**Fig. 4c**). This decrease trend with the increase of current density is due to the diffusion-limited charge/discharge process as well as the electrode overpotential at high current densities.[26] However, 84.5% of the SC at 1 A/g is still retained when the discharge current density is up to 8 A/g, which is comparable to or better than most of the Ni/carbon-based composite materials reported recently, such as peadot-like nickel@mesoporous carbon (912 F/g at 0.5 A/g),[25] hydrothermal synthesis of Ni@C core-shell structure (530 and 475 F/g at 1 and 3 A/g, respectively).[32]

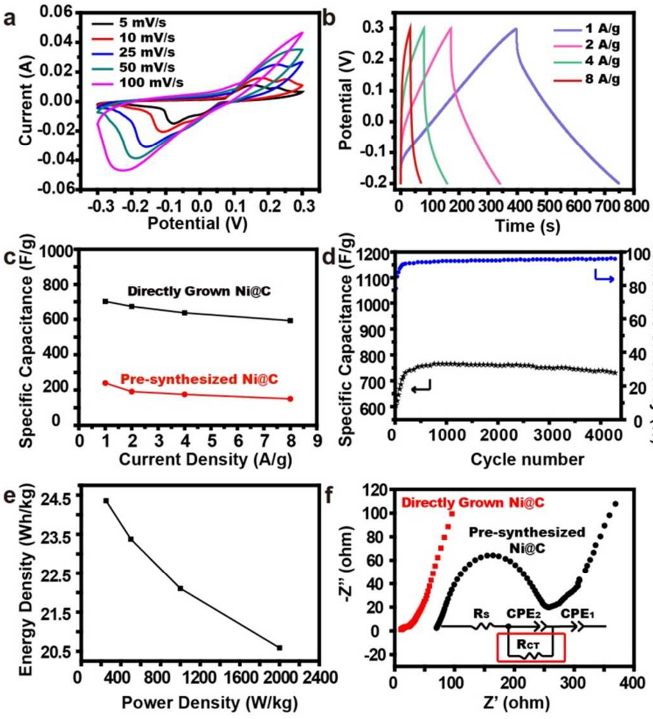

Figure 4. (a) Cyclic voltammetry of the mesoporous Ni@C composite directly grown on carbon fiber. Scan rates are 5, 10, 25, 50, 100 mV/s in 6 M KOH. (b) Charge-discharge curves of the mesoporous Ni@C composite at current densities of 1, 2, 4 and 8 A/g. (c) Specific capacitance with respect to the current density of the mesoporous Ni@C composites directly grown on carbon fibers (black curve) versus the post-coating of pre-synthesized mesoporous Ni@C on carbon fibers (red curve). (d) Cycling performance of the mesoporous Ni@C composite at a current density of 1 A/g. The capacitance and the Coulombic efficiency are displayed in black and blue curves. (e) Ragone plot relating power density to achievable energy density of the hybrid supercapacitor. (f) Nyquist plots of the mesoporous Ni@C composites directly grown on carbon fibers (red curve) versus the post-coating of pre-synthesized mesoporous Ni@C on carbon fibers (black curve). Inset shows the equivalent circuit.

In contrast, the post-coating of pre-synthesized Ni@C composite on carbon fibers using conventional adhesive reagents and carbon black shows only 150 F/g at 8 A/g, corresponding to around 62.5% retention at 1 A/g. This good electrochemical performance can be attributed to: i) the direct growth of the mesoporous Ni@C composite on the flexible CCB treated CFs with stable adhesion, which enables intimate contacts, short ion-diffusion length and effective electron transport between the charge collecting substrates and every mesoporous Ni@C composite; ii) loose textures of substrates and ample open spaces between neighboring composites achieving efficient impregnation of the electrolyte. Furthermore, our synthesis approach consists of only one single coating-calcination step, which is convenient and readily to scale up.

The cycling stability is further interrogated to demonstrate the potential of our mesoporous Ni@C composite for long-term use. At a current density of 1 A/g, the capacitance gradually increases from 603 to 740 F/g at the first 500 cycles (**Fig. 4d**), corresponding to 123% of its original value, which is possibly due to the activation process of the Ni-based electrodes.[25,33] After this increase, the specific capacitance is retained at ~ 740 F/g for over 4500 cycles with a negligible specific capacitance decay, demonstrating its superior cyclic stability performance. The Coulombic efficiency is also maintained over 95%, indicating that the perfectly mesoporous Ni@C composite supported by carbon textiles form a stable conductive structure and that the Faradaic redox reactions is reversible. Such significant electrochemical stability is comparable to or better than most works reported in the literature.[25,34] The energy density and power density of the overall electrode are two other critical parameters for practical applications. Judged by the Ragone plot (**Fig. 4e**), the highest energy density is about 24.4 Wh/kg with a power density of about 250 W/kg, and still retains above 20.6 Wh/kg at 2000 W/kg. These values are comparable with some of the previous work for analogous electrode systems[35,36] but can still be improved.

To confirm the enhanced charge transport by the carbon coating, the electrochemical impedance spectroscopy (EIS) is carried out for the mesoporous Ni@C composite directly grown on carbon fibers (**Fig. 4f**), compared to that of the post-coating of pre-synthesized Ni@C composite on carbon fibers using conventional adhesive reagents and carbon black. The Nyquist plots are recorded at a frequency range of 0.01 Hz–100 kHz at amplitude of 10 mV. The x-intercept represents the total electric series resistance, which is a combination of the electrolyte resistance, contact resistance at interface, and the intrinsic resistance of the electrode. The electric series resistances obtained by complex non-linear least square fitting is all calculated, based on an equivalent circuit. The mesoporous Ni@C composite directly grown on CCB treated CFs exhibits 5.7 and 2.2 Ω for R_s and R_{ct}, respectively, whereas the post-coating of pre-synthesized Ni@C composite on carbon fibers shows 60.7 and 141.1 Ω corresponding to R_s and R_{ct}. For the mesoporous Ni@C composite directly grown on CCB treated CFs, the steeper line in the low frequency range indicates the nearly ideal capacitor behavior. The straight line part of the curve is called Warburg resistance and the shorter line correlates to the shorter variations in ion diffusion path and more efficient charge transfer process for superior ionic conductivity at the electrode/electrolyte interface. However, pre-synthesized Ni@C composite exhibits a much larger diameter of the depressed semicircle, indicating the higher pseudocharge transfer resistance, which is related to the surface are and electrical conductivity. This result suggests that the direct growth of mesoporous Ni@C composite leads to a faster charge transfer process than the post-coating of pre-synthesized powers.

Finally, the mechanical stability of the mesoporous Ni@C composite on carbon fiber is demonstrated by measuring of electrochemical performance after repeated folding (**Fig. 5b**). The specific capacitance is retained almost constant (~ 99%), even after being folded with an angle of almost 180° for 70 times. Solid-state polymer electrolyte is further utilized to prove the flexibility of the electrode.[37] Polymer electrolyte with a limited amount of water can not only avoid leakage of electrolyte, but also mechanically stabilize the mesoporous Ni@C composite by retaining their structures and contacts during the cycling. Besides, solid-state device boosts considerable merits such as enhanced safety, ease of handling, scalability flexibility, and large range of operation temperature and so forth.[38] Thus, solid-state AC//Ni@C ASCs is developed by sandwiching PVA/KOH based solid-state electrolyte between a Ni@C on CCB treated CF-based cathode and an AC based anode.(**Fig. 5a**)

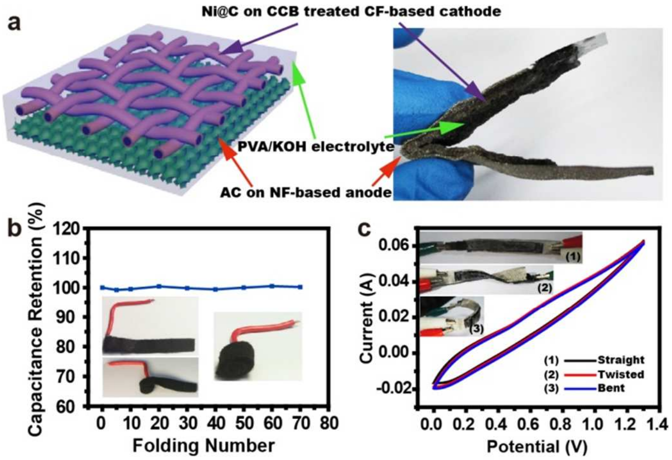

Figure 5. (a) A schematic diagram of a solid-state AC//Ni@C ASC with PVA/KOH polymer as the electrolyte and separator.(Left) Digital photograph of a bent AC//Ni@C ASC. (Right) (b) Stability test of the single electrodes mesoporous Ni@C composite upon repeated folding cycles. Insets: photographs of the mesoporous Ni@C composite electrodes on different folding states. (c) CV curves collected for ASC device under straight, twisted and bent conditions. Insets are the device pictures under test conditions.

The AC-based electrode exhibits a specific capacitance of ~120 F/g at a discharge current of 1 A/g (**Fig. S4**). The as-fabricated AC//Ni@C ASCs are highly flexible and have a low thickness of ~3 mm (**Fig. 5a**). In addition, no obvious decrease in the electrochemical performance has been detected in these ASCs when they are twisted and bent. The CV curves under straight, twisted and bent conditions are collected (**Fig.5c and inset**) and they are well maintained at a scan rate of 50 mV/s. These combined results of single electrodes and solid-state AC//Ni@C ASCs suggest that the direct growth of mesoporous Ni@C composite on flexible conducting substrates present remarkable electrochemical and mechanical stability.

Conclusions

In summary, we have put forward a facile one-pot approach for direct growth of mesoporous carbon-coated nickel nanoparticles on conductive carbon blacks treated carbon fibers as supercapacitors. The mesoporous Ni@C composite boosts a series of merits including a large mesopores of 5–30 nm for electrolyte access, large surface area of 71 m^2/g for effective electrochemical reactions, fast charge transfer pathways due to the highly conductive Ni nanoparticles and ultrathin carbon layer surface coating. These features are beneficial for electrochemical energy storage. As a proof-of-concept, supercapacitor electrodes fabricated from this mesoporous Ni@C composite exhibits a high capacitance of ~ 700 F/g at 1 A/g charge/discharge current density, with superior cycling stability over repeated folding cycles for single electrodes and excellent mechanical stability of different twisted and bent state for solid-state active carbon(AC)//Ni@C asymmetric supercapacitors. This growth method allows for further development of other carbon-coated hybrid nanocomposites with metals or metal oxides for efficient and flexible electrochemical energy storage.

Acknowledgements

We thank the following funding agencies for supporting this work: the National Key Basic Research Program of China (2013CB934104), the Natural Science Foundation of China (21322311, 21473038, 21071033), the Science and Technology Commission of Shanghai Municipality (14JC1490500), the Doctoral Fund of Ministry of Education of China (20130071110031), the Program for Professor of Special Appointment (Eastern Scholar) at Shanghai Institutions of Higher Learning, and the Deanship of Scientific Research of King Saud University (IHCRG#14-102). J.L. acknowledges the support of the Wang-Dao Undergraduate Research Funding of Fudan University.

Notes and references

[a] *Laboratory of Advanced Materials, Department of Chemistry, Fudan University, Shanghai, 200433, China.* [b] *School of Pharmacy, Fudan University, Shanghai, 201203, China. E-mail: gfzheng@fudan.edu.cn.*

† Electronic Supplementary Information (ESI) available: See DOI: 10.1039/b000000x/

1 Y. Tang, Y. Zhang, J. Deng, J. Wei, T. Hong Le, B. K. Chandran, Z. Dong, Z. Chen and X. Chen, *Adv. Mater.*, 2014, **26**, 6111-6118.

2 G. Zhang, H. B. Wu, T. Song, U. Paik and X. W. Lou, *Angew. Chem. Int. Ed.*, 2014, **53**, 1-5.

3 C. J. Niu, J. S. Meng, C. H. Han, K. N. Zhao, M. Y. Yan and L. Q. Mai, *Nano Lett.*, 2014, **14**, 2873-2878.

4 Y. Zhao, J. Feng, X. Liu, F. Wang, L. Wang, C. Shi, L. Huang, X. Feng, X. Chen, L. Xu, M. Yan, Q. Zhang, X. Bai, H. Wu and L. Mai, *Nat. Commun.*, 2014, **5**, 5565.

5 H. Wang, B. Zhu, W. Jiang, Y. Yang, W. R. Leow, H. Wang and X. Chen, *Adv. Mater.*, 2014, **26**, 3638-3643.

6 L. Liu, Z. Niu, L. Zhang, W. Zhou, X. Chen and S. Xie, *Adv. Mater.*, 2014, **26**, 4855-4862.

7 P. Yang, Y. Ding, Z. Lin, Z. Chen, Y. Li, P. Qiang, M. Ebrahimi, W. Mai, C. P. Wong and Z. L. Wang, *Nano Lett.*, 2014, **14**, 731-736.

8 L. Hu, J. W. Choi, Y. Yang, S. Jeong, F. La Mantia, L. F. Cui and Y. Cui, *Proc. Natl. Acad. Sci. U. S. A.*, 2009, **106**, 21490-21494.

9 W.-w. Liu, X.-b. Yan, J.-w. Lang, C. Peng and Q.-j. Xue, *J. Mater. Chem.*, 2012, **22**, 17245-17253.

10 X. Xue, P. Deng, B. He, Y. Nie, L. Xing, Y. Zhang and Z. L. Wang, *Adv. Energy Mater.*, 2014, **4**, DOI: 10.1002/aenm.201301329.

11 C. Meng, C. Liu, L. Chen, C. Hu and S. Fan, *Nano Lett.*, 2010, **10**, 4025-4031.

12 F. Meng and Y. Ding, Adv. Mater., 2011, 23, 4098-4102.

13 X. Lu, M. Yu, G. Wang, T. Zhai, S. Xie, Y. Ling, Y. Tong and Y. Li, *Adv. Mater.*, 2013, 25, 267-272.

14 X. Zhang, W. Shi, J. Zhu, W. Zhao, J. Ma, S. Mhaisalkar, T. L. Maria, Y. Yang, H. Zhang, H. H. Hng and Q. Yan, *Nano Res.*, 2010, **3**, 643-652.

15 Y. Xia, W. Zhang, Z. Xiao, H. Huang, H. Zeng, X. Chen, F. Chen, Y. Gan and X. Tao, *J. Mater. Chem.*, 2012, **22**, 9209-9215.

16 G. Yu, L. Hu, N. Liu, H. Wang, M. Vosgueritchian, Y. Yang, Y. Cui and Z. Bao, *Nano Lett.*, 2011, **11**, 4438-4442.

17 Q. Li, J. Sheng, Q. Wei, Q. An, X. Wei, P. Zhang and L. Mai, *Nanoscale*, 2014, **6**, 11072-11077.

18 L. Mai, F. Dong, X. Xu, Y. Luo, Q. An, Y. Zhao, J. Pan and J. Yang, *Nano Lett.*, 2013, **13**, 740-745.

19 H. Wang, H. S. Casalongue, Y. Liang and H. Dai, *J. Am. Chem. Soc.*, 2010, **132**, 7472-7477.

20 D. Qiu, Z. Xu, M. Zheng, B. Zhao, L. Pan, L. Pu and Y. Shi, *J. Solid State Electrochem.*, 2012, **16**, 1889-1892.

21 H. B. Wu, H. Pang and X. W. Lou, *Energy Environ. Sci.*, 2013, **6**, 3619-3626.

22 L. Huang, D. Chen, Y. Ding, S. Feng, Z. L. Wang and M. Liu, *Nano Lett.*, 2013, **13**, 3135-3139.

23 L. Shen, Q. Che, H. Li and X. Zhang, *Adv. Funct. Mater.*, 2014, **24**, 2630-2637.

24 S.-M. Bak, K.-H. Kim, C.-W. Lee and K.-B. Kim, *J. Mater. Chem.*, 2011, **21**, 1984-1990.

25 H. Jiang, T. Sun, C. Li and J. Ma, *RSC Adv.*, 2011, **1**, 954-957.

26 T. Wang, Z. Peng, Y. Wang, J. Tang and G. Zheng, *Sci. Rep.*, 2013, **3**, 2693

27 Z. Y. Hou, O. Yokota, T. Tanaka and T. Yashima, *Appl. Catal., A*, 2003, **253**, 381-387.

28 K. W. Nam and K. B. Kim, *J. Electrochem. Soc.*, 2002, **149**, A346-A354.

29 V. Ganesh, V. Lakshminarayanan and S. Pitchumani, *Electrochem. Solid-State Lett.*, 2005, **8**, A308-A312.

30 T. Liu, G. Shao and M. Ji, *Mater. Lett.*, 2014, **122**, 273-276.

31 S. Vijayakumar, S. Nagamuthu and G. Muralidharan, *ACS Sustainable Chem. Eng*, 2013, **1**, 1110-1118.

32 L. Niu, Z. Li, J. Sun, Z. Fan, Y. Xu, P. Gong, S. Yang and J. Wang, *J. Alloys Compd.*, 2013, **575**, 152-157.

33 L. F. Shen, Q. Che, H. S. Li and X. G. Zhang, *Adv. Funct. Mater.*, 2014, **24**, 2630-2637.

34 C. Wu, S. Deng, H. Wang, Y. Sun, J. Liu and H. Yan, *ACS Appl. Mater. Interfaces*, 2014, **6**, 1106-1112.

35 Z. Yang, C.-Y. Chen and H.-T. Chang, *J. Power Sources*, 2011, **196**, 7874-7877.

36 H. Inoue, Y. Namba and E. Higuchi, *J. Power Sources*, 2010, **195**, 6239-6244.

37 X. Lu, G. Wang, T. Zhai, M. Yu, S. Xie, Y. Ling, C. Liang, Y. Tong and Y. Li, *Nano Lett.*, 2012, **12**, 5376-5381.

38 Z. Tang, C.-h. Tang and H. Gong, *Adv. Funct. Mater.*, 2012, **22**, 1272-1278.

Graphical Abstract

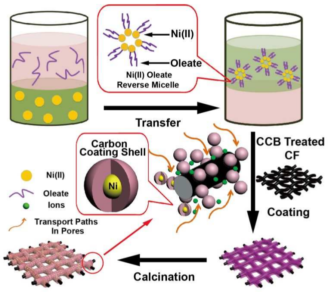

A solution method for direct growth of mesoporous carbon-coated nickel nanoparticles on carbon fibers is demonstrated for flexible supercapacitors.